SCIENCE CHINA
Earth Sciences

• RESEARCH PAPER •

November 2013 Vol.56 No.11: 1918–1925
doi: 10.1007/s11430-013-4658-6

Reaction experiments between tonalitic melt and mantle olivine and their implications for genesis of high-Mg andesites within cratons

WANG MingLiang[1,2] & TANG HongFeng[1*]

[1] *Laboratory for High Temperature & High Pressure Study of the Earth's Interior, Institute of Geochemistry, Chinese Academy of Sciences, Guiyang 550002, China;*
[2] *University of Chinese Academy of Sciences, Beijing 100049, China*

Received October 28, 2012; accepted March 27, 2013; published online July 25, 2013

High-Mg (Mg#>45) andesites (HMA) within cratons attract great attention from geologists. Their origin remains strongly debated. In order to examine and provide direct evidence for previous assumptions about HMA's genesis inferred from petrological and geochemical investigations, we performed reaction experiments between tonalitic melt and mantle olivine on a six-anvil apparatus at high-temperature of 1250–1400°C and high-pressure of 2.0–5.0 GPa. Our experiments in this work simulated the interaction between the tonalitic melt derived from partial melting of eclogitized lower crust foundering into the Earth's mantle and mantle peridotite. The experimental results show that the reacted melts have very similar variations in chemical compositions to the HMAs within the North China Craton. Therefore, this interaction is probably an important process to generate the HMAs within crations.

tonalitic melt, mantle olivine, melt-mineral reaction experiment, high-Mg andesite, craton

Citation: Wang M L, Tang H F. Reaction experiments between tonalitic melt and mantle olivine and their implications for genesis of high-Mg andesites within cratons. Science China: Earth Sciences, 2013, 56: 1918–1925, doi: 10.1007/s11430-013-4658-6

Andesite, a type of calc-alkaline lava with SiO_2 content of 52 wt%–65 wt%, is widely found in active continental margins. Andesite has derived its name from its typical occurrence in the Andes. One type of andesites with high-Mg content is called high-Mg andesite, HMA for short. This type of andesites can be found both in convergent plate margins and within plates. The HMAs occurring in convergent plate margins such as island arc and active continental margin are characterized by relatively low MgO content and Mg# (less than 10 wt% and >30, respectively) (Kelemen, 1995). Previous geochemical (Shimoda et al., 1998; Pearce et al., 1992) and experimental (Johnston et al., 1989; Rapp et al., 1999) investigations have shown that the interaction between hydrous melts and mantle wedge could account for their generation. However, the HMAs occurring within plates, such as those within the North China Craton (Gao et al., 2004; Huang et al., 2007; Wu et al., 2003; Xu et al., 2006; Yuan et al., 2005; Xu et al., 2008; Wang et al., 2005; Zhang et al., 2003; Xiong et al., 2011), have relatively high MgO content and Mg# (>45). Detailed petrological and geochemical studies have suggested that the original magma forming these HMAs is that formed by partial melting of eclogitized lower crust foundering into the Earth's mantle, and contaminated by mantle rocks (Gao et al., 2004; Huang et al., 2007; Xu et al., 2008); or that formed by partial melting of lithospheric mantle that has been previously metasomatized by adakitic melt derived from subducted crust (Wu et al., 2003).

*Corresponding author (email: tanghongfeng@vip.gyig.ac.cn)

In contrast with the plate margin rich in water, the lithospheric mantle beneath craton has much lower water content (Xie et al., 2005). As water content directly affects and constrains the order and *P-T* ranges of mineral crystallization, the results from previous experiments pertaining to the origin of HMAs at the conditions corresponding to plate margins are not fully applicable to the HMAs within cratons. Previous experimental researches on the genesis of HMAs within cratons were only reported in Yu et al. (2009) and Wang et al. (2010). Yu et al. (2009) performed experiments using a basaltic starting melt. Wang et al. (2010) carried out reaction experiments between a peridotite and variable andesitic melts at a constant pressure (2.0 GPa) and different temperatures. However, in the mantle beneath craton, the melt derived from partial melting of the delaminating eclogite is generally determinate, and during its upwelling, the melt will react with mantle peridotites under varying temperature and pressure conditions. Therefore, it is difficult for these researches to provide appropriate solutions for the following two issues: (1) How does magma with relatively fixed composition evolve into HMA under different temperature and pressure conditions; (2) How do temperatures and pressures affect the composition of magma forming HMA. In order to completely explore the interaction of an andesitic melt with mantle olivine/peridotite at variable temperatures and pressures, and to examine previous assumptions about HMA's genesis inferred from petrological and geochemical investigations, we performed reaction experiments between tonalitic melt and mantle olivine under high-temperature and high-pressure conditions.

1 Experimental and analytical methods

1.1 Starting materials

Based on the suggestions from Gao et al. (2008, 2009) that the magma generated by partial melting of the eclogitized lower crust foundering in the Earth's mantle is tonalitic to trondhjemitic or adakitic, a tonalite was chosen as the starting material to prepare melt glass, which was collected from Sandouping of Huangling, Hubei, China and kindly provided by Prof. Zhou Hanwen at China University of Geosciences. Its composition is given in Table 1. The mantle olivine was separated from a mantle lherzolite xenolith occurring in the Hannuoba Cenozoic basalt and kindly supplied by Prof. Xie Hongsen. Its composition is also listed in Table 1. The homogeneous tonalitic glass was prepared by crushing chips of the tonalite, ultrasonic washing with distilled water and ethanol, grinding manually in an agate mortar to a ~200 mesh powder, melting three times in a Fe-saturated Pt crucible at 1500°C and 1atm for an hour, and quenching. As shown in Table 1, the tonalitic glass has the same chemical composition as the tonalite. The pure olivine grains were prepared by crushing of the lherzolite xenolith to ~20 mesh separates, handpicking under a binocular microscope, and ultrasonic washing with deionzied water and ethanol.

1.2 Temperature and pressure conditions

The temperatures for the reaction experiments in this study have been designed at 1250–1400°C by taking into account the following aspects: (1) During the Mesozoic, the eruption-time of the HMAs within the North China Craton, the temperature at depth of 100 km (corresponding to about 3.0 GPa) was approximate to 1300–1350°C (Xu, 2001), and the temperature fluctuation was about 100°C (Anderson, 2000). (2) The upper thermal stability of lherzolite is 1450°C at 3.0 GPa (Anderson, 2005), which implies that olivine is stable as solid below this temperature at 3.0 GPa. (3) The phase diagram in Sekine et al. (1982) and the result calculated by using the software from the website of Melts at (http://melts.ofm-research.org/Applet/applet_download. html) suggest that the tonalite we used will be completely melted when temperature exceeds 1250°C at 3.0 GPa. By considering that the melt probably interacts with mantle peridotite in a range of depth during its movement, hence we have designed the pressures at 2.0–5.0 GPa. The detailed experimental *P-T* conditions in this paper are shown in Table 2.

1.3 Experimental procedure

All the reaction experiments in this paper were performed using the JL-3600 six-anvil apparatus equipped at the Laboratory for High Temperature & High Pressure Study of the Earth's Interior, Institute of Geochemistry, Chinese Academy of Sciences. The starting materials, tonalitic glass powder and olivine, were loaded in a Pt capsule with 6 mm in inner diameter and 6 mm long using an interbedded man-

Table 1 Chemical compositions (wt%) of the starting materials[a)]

	SiO_2	TiO_2	Al_2O_3	FeO	MnO	MgO	CaO	Na_2O	K_2O	P_2O_5	Total	Mg#
Tonalite	64.09	0.46	17.54	4.61	0.11	2.83	4.62	4.14	1.40	0.18	100.00	52
Tonalitic glass	64.76	0.46	17.29	4.70	0.12	2.79	4.39	3.88	1.44	0.17	100.00	51
Olivine	42.24	0.02	0.28	8.64	0.19	48.71	0.00	0.00	0.00	0.00	100.08	91

a) The data of the tonalite and tonalitic glass are recalculated to 100 wt% anhydrous from primary XRF results. The losses on ignition for the tonalite and tonalitic glass are 2.05 wt% and 1.75 wt%, respectively; and the total iron was expressed as FeO. The data of the mantle olivine are from Gong et al. (2011).

Table 2 Experimental conditions and phase assemblages of the run products[a)]

Run No.	Temperature (°C)	Pressure (GPa)	Duration (h)	Phase assemblage
DD-03	1250	3.0	72	Ol+Gl+Opx+Grt+Cpx
DD-02	1300	3.0	72	Ol+Gl+Opx+Grt
DD-04	1350	3.0	72	Ol+Gl+Opx
DD-05	1400	3.0	72	Ol+Gl+Opx
DD-06	1350	2.0	58	Ol+Gl+Opx
DD-04	1350	3.0	72	Ol+Gl+Opx
DD-07	1350	4.0	46	Ol+Gl+Opx
DD-08	1350	5.0	72	Ol+Gl+Opx+Grt

a) Phase abbreviation: Ol=olivine, Gl=melt, Opx=orthopyroxene, Grt=garnet Cpx=clinopyxene. Note that the first two phases are the reacted starting materials, and the last three are the newly formed and constituent minerals in reaction rims.

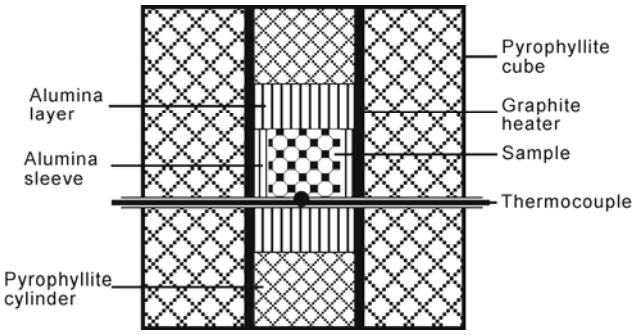

Figure 1 Sketch map showing the sample assemblage for the experiments in this study.

ner, which was constructed by three glass layers and two olivine ones. The loaded capsule was filled in a thin-walled (1 mm) Al_2O_3 sleeve, and these two parts then were placed in a graphite heater, which was plugged by calcined pyrophyllite cylinder at both ends. The detailed sample assemblage for the experiments is shown in Figure 1. Based on the weights of the starting materials loaded in the capsule, the proportion of melt relative to olivine in each run was determined and controlled in the range of 0.8∶1 to 1∶1, suggesting that the starting composition was approximately consistent in each run. The above-mentioned proportions resulted in the experiments oversaturated with olivine, and the reaction rims preserved facilely and observed clearly. The temperature was measured and controlled using $PtRh_6$-$PtRh_{30}$ thermocouples, and accurate to $<\pm5$°C. According to the long-term monitoring results from Zhu Chengming on the six-anvil apparatus (Fu et al., 1985), the temperature gradient in the sample chamber of this study is about 6°C. The pressure was accurate to $<\pm0.3$ GPa. In a single run, the pressure was first raised to the desired value, and then the temperature was increased to the desired value by three steps. Finally, the experiment was held at the desired temperature and pressure conditions. After the designed duration, the experimental charge was quenched by turning power off, and then the run product was removed carefully from the capsule and mounted in epoxy, which was polished for observation and electron microprobe analysis.

1.4 Sample analysis

The chemical compositions of the tonalite and its glass were analyzed on an Axios (PW4400) X-ray fluorescence (XRF) spectrometer at the State Key Laboratory of Ore Deposit Geochemistry, Institute of Geochemistry, Chinese Academy of Sciences. The results are listed in Table 1. The chemical compositions of the run products were determined on a JOEL JXA-8100 electron microprobe at the State Key Laboratory for Mineral Deposits Research, Nanjing University. The accelerating potential was 15 kV. The standard samples used were from the U.S. National Bureau of Standards, and the relative error does not exceed 3%. The detailed procedure can be referred to Zhang et al. (2011), The results are listed in Table 3.

2 Experimental results

The phase assemblages of the run products are listed in Table 2, and the representative backscattered electron (BSE) images are shown in Figure 2. The results display that orthopyroxene (Opx) is the primary mineral newly formed and occurring around olivine in all reaction experiments in this study (Figure 2). Garnet (Grt) is favorably developed at relatively lower temperature and higher pressure conditions, and it occurs close to Opx (Figure 2(a), (b) and (d)). Clinopyroxene (Cpx) is formed only at 3.0 GPa and 1250°C, and occurs at the outmost side of the reaction rim and close to the melt (Figure 2(a)). Together with formation of the new minerals, the chemical compositions of the starting materials have also been changed to some extent.

2.1 Compositional variation in starting materials

The chemical composition of the starting melt has been modified after the reaction. With increasing temperatures, MgO contents of the reacted melts are increased and have a positively linear relationship with temperature (Figure 3(g)), whereas SiO_2, Al_2O_3, and K_2O contents in the reacted melt are linearly decreased (Figure 3(e), (f), and (h)). The influence of pressure on the chemical composition of the reacted

Table 3 Chemical compositions (wt%) of the run products[a)]

Reacted melt								
Pressure (GPa)	2.0	3.0	4.0	5.0	3.0	3.0	3.0	3.0
Temperature (°C)	1350	1350	1350	1350	1250	1300	1350	1400
Analysis spot	5	7	8	5	7	6	7	5
SiO_2	60.34(0.26)	65.76(1.99)	66.30(1.27)	66.21(0.88)	71.02(0.89)	69.60(0.93)	65.76(1.99)	62.13(1.77)
TiO_2	0.38(0.02)	0.40(0.05)	0.38(0.04)	0.39(0.04)	0.48(0.02)	0.43(0.03)	0.40(0.05)	0.39(0.02)
Al_2O_3	15.95(0.19)	17.00(0.41)	16.55(0.67)	17.12(0.26)	18.53(0.21)	17.86(0.48)	17.00(0.41)	15.54(0.37)
FeO	5.92(0.08)	0.17(0.03)	0.20(0.04)	0.17(0.05)	0.83(0.1)	0.33(0.08)	0.17(0.03)	2.67(0.13)
MnO	0.14(0.02)	0.08(0.02)	0.05(0.02)	0.08(0.02)	0.06(0.03)	0.05(0.02)	0.08(0.02)	0.12(0.03)
MgO	9.75(0.29)	8.71(1.47)	8.83(0.45)	7.92(0.81)	1.66(0.07)	3.93(0.77)	8.71(1.47)	11.94(0.71)
CaO	4.28(0.07)	4.39(0.43)	4.52(0.08)	4.56(0.08)	4.08(0.06)	4.71(0.08)	4.39(0.43)	4.52(0.09)
Na_2O	2.32(0.17)	1.53(0.56)	2.18(0.37)	2.04(0.05)	1.61(0.16)	1.72(0.16)	1.53(0.56)	1.44(0.65)
K_2O	1.10(0.03)	1.03(0.19)	1.10(0.22)	0.94(0.22)	1.67(0.05)	1.35(0.07)	1.03(0.19)	0.91(0.06)
P_2O_5	0.15(0.02)	0.18(0.02)	0.17 (0.02)	0.18(0.02)	0.22(0.03)	0.20(0.02)	0.18(0.02)	0.17(0.01)
Total	100.39(0.29)	99.28(0.61)	100.28(0.98)	99.64(0.36)	100.17(0.81)	100.19(0.70)	99.28(0.61)	99.90(1.04)
Reacted olivine								
Pressure (GPa)	2.0	3.0	4.0	5.0	3.0	3.0	3.0	3.0
Temperature (°C)	1350	1350	1350	1350	1250	1300	1350	1400
Analysis number	5	7	10	7	5	3	7	5
SiO_2	40.88(0.34)	40.52(0.47)	41.06(1.22)	39.90(1.87)	40.17(0.18)	40.49(0.61)	40.52(0.47)	39.91(1.46)
FeO	9.48(0.23)	10.39(0.72)	10.35(0.36)	10.46(0.53)	11.16(0.12)	10.87(0.35)	10.39(0.72)	9.55(0.17)
MnO	0.13(0.02)	0.15(0.04)	0.13(0.02)	0.12(0.03)	0.13(0.02)	0.14(0.02)	0.15(0.04)	0.12(0.03)
MgO	48.41(1.03)	48.33(0.68)	48.13(1.42)	48.82(0.68)	47.69(1.11)	48.40(0.73)	48.33(0.68)	49.63(0.69)
CaO	0.04(0.01)	0.03(0.02)	0.05(0.01)	0.01(0.02)	0.02(0.01)	0.02(0.01)	0.03(0.02)	0.02(0.01)
NiO	0.41(0.03)	0.38(0.02)	0.34(0.05)	0.40(0.06)	0.37(0.02)	0.40 (0.02)	0.38(0.02)	0.49(0.03)
Total	99.36(0.08)	99.80(0.62)	100.05(0.48)	99.71(1.27)	99.54(1.11)	100.31(0.92)	99.80(0.62)	99.72(0.82)
Mg#	90(0)	89(0)	89(1)	89(0)	88(0)	89(0)	89(0)	90(1)
Orthopyroxene								
Pressure (GPa)	2.0	3.0	4.0	5.0	3.0	3.0	3.0	3.0
Temperature (°C)	1350	1350	1350	1350	1250	1300	1350	1400
Analysis spot	5	4	4	4	2	3	4	4
SiO_2	55.11(1.17)	57.60(0.43)	57.92(0.58)	58.02(0.45)	55.42(0.14)	56.74(0.79)	57.60(0.43)	56.69(1.44)
TiO_2	0.06(0.03)	0.06(0.03)	0.04(0.04)	0.05(0.05)	0.23(0.04)	0.08(0.08)	0.06(0.03)	0.03(0.02)
Al_2O_3	3.84(0.34)	3.73(0.71)	5.36(0.92)	2.09(0.29)	2.70(0.93)	3.54(1.60)	3.73(0.71)	2.81(0.28)
FeO	6.20(0.80)	1.65(2.01)	0.97(0.53)	4.48(1.34)	7.86(0.66)	3.24(1.96)	1.65(2.01)	4.90(0.36)
MnO	0.15(0.03)	0.15(0.02)	0.11(0.02)	0.12(0.03)	0.15(0.04)	0.12(0.06)	0.15(0.02)	0.10(0.03)
MgO	33.71(0.73)	35.23(0.36)	33.83(0.36)	34.07(0.03)	31.87(1.00)	34.38(1.61)	35.23(0.36)	34.23(0.94)
CaO	0.52(0.11)	0.61(0.26)	0.91(0.10)	0.25(0.54)	0.63(0.04)	0.64(0.21)	0.61(0.26)	0.39(0.28)
Na_2O	0.10(0.05)	0.21(0.09)	0.41(0.03)	0.11(0.20)	0.08(0.05)	0.12(0.06)	0.21(0.09)	0.15(0.09)
NiO	0.17(0.02)	0.06(0.06)	0.04(0.04)	0.16 (0.01)	0.17(0.04)	0.11(0.03)	0.06(0.06)	0.13(0.03)
Cr_2O_3	0.12(0.08)	0.16(0.06)	0.07(0.03)	0.04(0.02)	0.02(0.02)	0.06(0.04)	0.16(0.06)	0.13(0.10)
Total	99.97(0.59)	99.45(0.68)	99.67(0.59)	99.37(0.84)	99.11(1.43)	99.03(1.29)	99.45(0.68)	99.54(0.29)
En	91	97	98	93	88	95	97	93

	Clinopyxene		Garnet		
Pressure (GPa)	3.0		5.0	3.0	3.0
Temperature (°C)	1250		1350	1250	1300
Analysis spot	4		7	7	3
SiO_2	51.86(0.37)		40.59(0.71)	40.83(1.15)	40.71(0.07)
TiO_2	0.54(0.05)		0.12(0.03)	0.39(0.05)	0.25(0.07)
Al_2O_3	17.72(0.16)		25.98(0.55)	24.48(0.44)	25.23(0.07)
FeO	4.41(1.64)		3.55(0.62)	8.98(2.25)	6.27(0.10)
MnO	0.15(0.03)		0.33(0.06)	0.49(0.05)	0.41(0.02)
MgO	8.28(0.59)		25.04(2.17)	18.50(2.50)	21.77(1.00)
CaO	13.22(1.31)		2.89(0.53)	6.27(1.46)	4.58(0.11)
Na_2O	3.84 (0.24)		0.04 (0.02)	0.07(0.02)	0.06(0.02)
Cr_2O_3	0.12(0.07)		0.41(0.10)	0.20(0.09)	0.31(0.04)
Total	100.23(0.39)		99.00(0.68)	100.34(0.67)	99.66(1.04)
Component	$Wo_{47}En_{41}Fs_{12}$	Pyr	85	65	76

a) Listed here are the averages of analysis spots, and the numbers in brackets refer to standard deviation: Mg#=molar 100×Mg/(Mg+ΣFe); En represents the percentage of enstatite component in orthopyroxene, and Pyr the percentage of pyrope component in garnet.

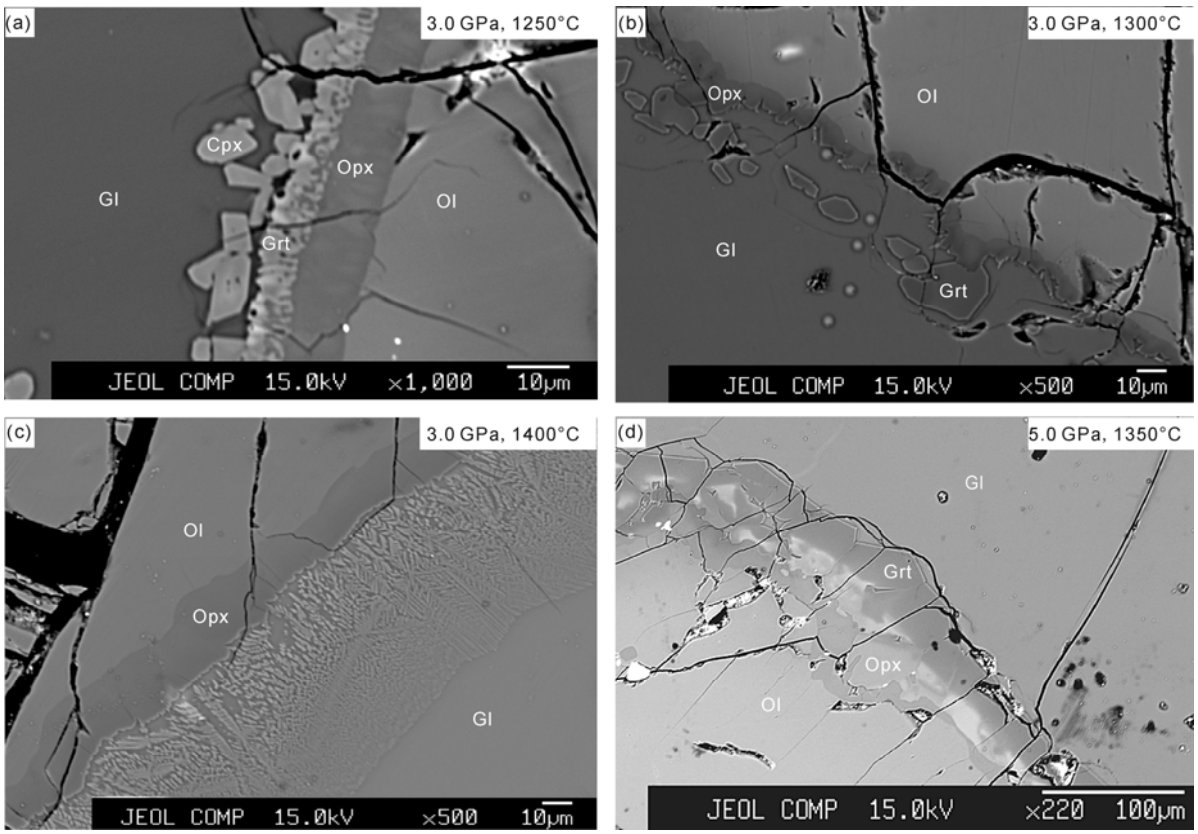

Figure 2 Representative BSE images of run products. The images display three types of reaction rim at the outside margin of the reacted olivine. From the order that newly formed minerals occur off the olivine, the reaction rims can be defined (Opx+Grt+Cpx)-type, (Opx+Grt)-type, and Opx-type. The first one only occurs at (1250°C, 3.0 GPa), the second one at (1300°C, 3.0 GPa) and (1350°C, 5.0 GPa), and the last one at any other conditions.

melt is not clear, and the compositional variations resulted from change in pressure are generally far less than from that in temperature. In all experiments, the reacted melts have higher Mg# (=molar 100×Mg/(Mg+ΣFe)) than that of the starting tonalite, and their CaO contents are in the range of 4.08 wt%–4.71 wt% (Table 3) and with an average of 4.44 wt% very close to those of the starting tonalite and its glass (Table 1). Compared with the reacted melts, which have relatively complicated variations in chemical composition, the reacted olivines have almost the same chemical compositions (Table 3) as the starting one (Table 1).

2.2 Chemical compositions of newly formed minerals

The orthopyroxenes occurring in all run products are Mg-rich enstatites defined by their compositions (Table 3). Their FeO contents, less than 10 wt%, and Mg# values are slightly different among runs. The garnets consist predominantly of pyrope component (Table 3). Their chemical compositions are not apparently affected by pressure, but primarily constrained by temperature. With increasing temperature, the FeO and CaO contents in the garnets decreased but MgO content increased. The clinopyroxene occurring only at 1250°C and 3.0 GPa is diopside as shown in Table 3.

3 Discussion

3.1 Reaction mechanism and equilibrium

In general, mechanisms of reactions between melt and solid mineral are involved principally in two processes: diffusion and dissolution-crystallization. Diffusion is element migration driven by chemical potential gradient due to concentration differences of elements between melt and mineral (Liang, 2010). Dissolution-crystallization is a sequential process. At first, solid mineral partially melts due to erosion by hot magma. The resulting melt then mixes with the hot magma and locally forms a mixed melt in which some components become oversaturated. Finally the mixing melt crystallizes new mineral(s) corresponding to the oversaturated components.

Diffusion has certainly occurred in our reaction experiments. The reacted melt with homogeneous composition in each experiment is attributed mainly to this process. However, diffusion is not the only and primary mechanism controlling the whole reaction process. As shown in Table 3, with temperature increased from 1250°C to 1400°C, the MgO contents in the reacted melts increased from 1.66 wt% to 11.94 wt%. When the starting melt is chosen as a reference, from the principle of diffusion, the increasing MgO

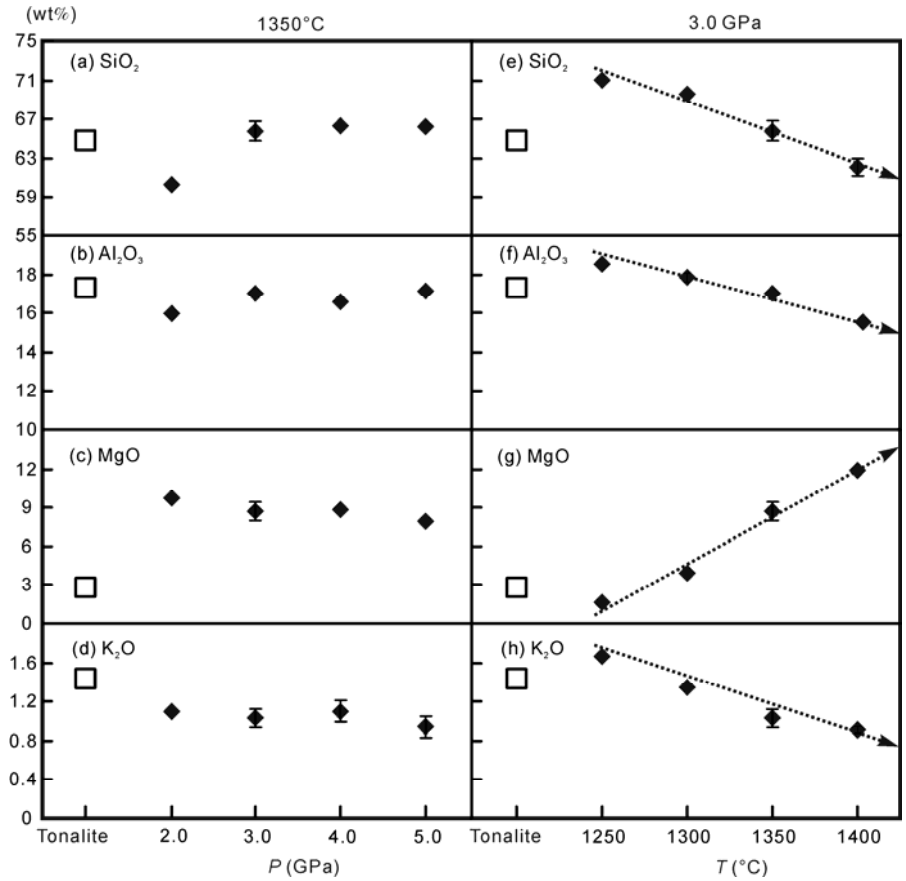

Figure 3 Compositional variations of the reacted melts. Shown in (a)–(d) are those at 1350°C with increasing pressures, and in (e) to (h) at 3.0 GPa with increasing temperatures. The starting tonalitic melt is shown as square.

contents in the reacted melt with increasing temperature suggest that more Mg from the olivine should have migrated into the melt correspondingly with decreasing MgO contents in the reacted olivines. However, the reacted olivines have almost no apparently compositional variation (Table 3). The diffusion is therefore not the primary mechanism in our reaction experiments. Then the other mechanism, dissolution-crystallization, is the crucial one. With temperature increased, more dissolved olivine contributes to the melt, resulting in that the melt has higher MgO content, and that the total mass of the melt is increased. Consequently, the SiO_2, Al_2O_3, and K_2O contents in the melts are relatively decreased due to dilution. As Al_2O_3 and K_2O are only rich in the starting melt in our experiments (Table 1), these two oxides in the reacted melts can be used to monitor the mass variations in the melts. With a continuous contribution from the dissolved olivine, the melts are continually modified. Once some components in the melt are oversaturated, new minerals corresponding to these components crystallize around olivine. In our experiments, the first crystallizing mineral is Opx. Its crystallization has prevented olivine from further dissolution. Other minerals such as Grt and Cpx likely crystallize after Opx when related components to these two minerals are oversaturated. (Opx+Grt+Cpx)-type (Figure 2(a)) or (Opx+Grt)-type (Figure 2(b) and (d)) reaction rims are therefore developed. If no other minerals formed after Opx, then the reaction rim is Opx-type (Figure 2(c)). From the above discussion, although both diffusion and dissolution-crystallization have contributed to the experimental results in this study, the latter has mainly controlled the chemical compositions in the reacted melts and olivines, and the mineral assemblages in the reaction rims and the chemical compositions of the newly formed minerals. Dissolution-crystallization should thus be the dominate mechanism for the reaction experiments studied.

In regard to equilibrium in our experiments, we consider that local equilibriums have achieved between the reaction rims and the melts or the olivines. According to the clinopyroxene thermometer in Xu (1993), we can estimate the temperature of the experiment with Cpx. The estimated result is 1254°C, quite in agreement with the desired temperature of 1250°C within error, suggesting that the equilibrium in this experiment has achieved. It is well known that reaction rate is positively dependent of temperature, and reaction equilibrium approaches facilely at higher temperature than lower one. As 1250°C is the lowest temperature desired in our experiments, then other experiments should also have approached equilibrium. The homogeneous re-

acted melt and olivine in each experiment also indicate that equilibrium has been achieved.

3.2 Comparison with previous experiments

In our experiments as shown in Table 2, the assemblages of the newly formed minerals in the reaction rims are orderly developed as follows: (1) Opx+Grt+Cpx (1250°C), Opx+Grt (1300°C), and Opx (1350°C and 1400°C) with temperature increased at 3.0 GPa, and (2) Opx (2.0; 3.0; 4.0 GPa) and Opx+Grt (5.0 GPa) with pressure increased at 1350°C. These results are similar to the mineral assemblage variations reported by Sekine et al. (1982) in a peridotite-dominate system, which the peridotite mass is more than 80% of the total. The difference between our results and those in Sekine et al. (1982) is that there is phlogopite in the low temperature field due to lower temperature and the water-bearing starting material in their experiments. Compared with the experimental results in Wang et al. (2010), the similarity is that orthopyroxenes have developed as the primary mineral around olivines in all experiments. The difference is that there is a large amount of clinopyroxenes in their experiments, but only has developed at 1250°C and 3.0 GPa (run DD-03) among ours. This difference is probably attributed to CaO contents in the starting melts. The CaO contents in the starting materials used by Wang et al. (2010) are 8 wt%–12 wt%, but it is only 4.59 wt% in our experiments. High CaO content in the starting material is beneficial to forming Ca-rich clinopyroxene (Wang et al., 2010). In addition, the compositional variations of the reacted melts in our run products compared with the starting melt we used are mainly obvious increases in MgO contents and Mg# values, which is consistent with those in previous peridotite- or olivine-bearing experiments (Johnston et al., 1989; Rapp et al., 1999; Yu et al., 2009; Wang et al., 2010; Sekine et al., 1982).

There is a possible Fe loss due to direct contact of the starting melts with Pt-capsules in our experiments. From the study of Grove (1981) and our unpublished results of the experiments between the tonalitic melt and mantle peridotite under the same conditions but no direct contact of the starting melt with Pt-capsules, the estimated Mg# values in the reacted melts in this study are likely around 80, and the Mg# values of the newly formed Opx are about 90–92. However, the Mg# values in the olivines are independent of the possible Fe loss.

3.3 Genesis of HMAs within cratons

The major-element compositions of the typical HMAs occurring in several places within the North China Craton (Gao et al., 2004; Huang et al., 2007; Wu et al., 2003; Xu et al., 2006; Yuan et al., 2005) display that their MgO and SiO_2 contents are negatively correlated (Figure 4). Compared to the starting melt, the reacted melts reported in this paper have increasing MgO contents and similarly negative MgO versus SiO_2 correlation (Figure 4). This similarity implies that the HMAs may have also experienced reactions between andesitic melt and olivine during their formation. The reacted melts with garnets in some experiments are possibly depleted in heavy rare earth elements and Y, which is applicable to explaining the origin of the high-Mg adakites within the North China Craton reported by Zhang et al. (2001) and Gao et al. (2004). Furthermore, the experimental results in this paper are in agreement with those reported by Liu et al. (2005) from case study, which is that orthopyroxene contents increase with olivine decreasing during the reactions between melts and mantle peridotites. In summary, from cross confirmation by experimental results and geological facts, we suggest that the reaction between andesitic melts and mantle olivines/perdotites is probably an important process to generate the HMAs within cratons.

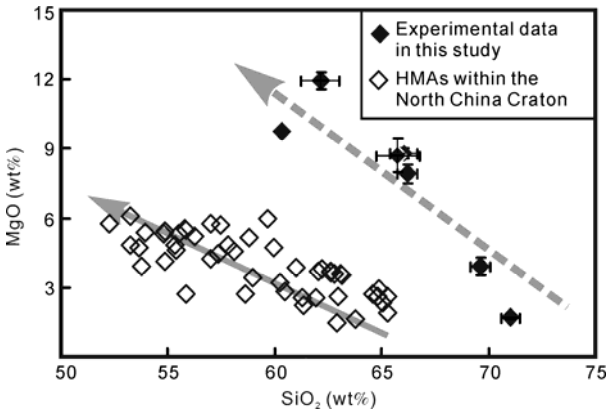

Figure 4 Comparison of MgO versus SiO_2 plots between the HMAs within the North China Craton. Data from references (Gao et al., 2004; Huang et al., 2007; Wu et al., 2003; Xu et al., 2006; Yuan et al., 2005) and the reacted melts in this study (data listed in Table 3). The plots of MgO versus SiO_2 for the reacted melts define a negative variation trend in agreement with that for the HMAs.

4 Conclusions

(1) The mechanisms of the reaction between the tonalitic melt and mantle olivine are element diffusion and dissolution of the olivine followed by crystallization of new minerals, and the dissolution-crystallization process is the dominant mechanism during the reaction studied.

(2) After the reaction between the tonalitic melt and mantle olivine, the reacted melt has increased MgO content and Mg# value, whereas the reacted olivine has nearly the same composition as that of the starting one.

(3) The magma forming the HMAs within cratons can be generated through the reaction between the melt derived from partial melting of foundering lower crust into the Earth's mantle and mantle olivine.

We thank Zhou Hanwen and Xie Hongsen for providing the starting materials, Li Chong for help in glass preparation, Zhu Chengming and Cai Enzhao for technical assistance in high-pressure apparatus operation, and Zhang Wenlan and Rao Can for support and help in electron microprobe analysis. Beneficial discussions with Zhou Wenge and valuable comments and suggestions from two anonymous reviewers are also gratefully acknowledged. We also thank Miao Desui for offering helpful suggestions during the English edition polishing. This work was financially supported by the Knowledge Innovation Program of the Chinese Academy of Sciences (Grant No. KZCX2-YW-Q08-3-4) and the project from the State Key Laboratory for Mineral Deposits Research, Nanjing University (Grant No. 15-09-08).

Anderson D L. 2000. The thermal state of the upper mantle: No role for mantle plumes. Geophys Res Lett, 27: 3623–3626

Anderson D L. 2005. Large igneous provinces, delamination, and fertile mantle. Elements, 1: 271–257

Fu H F, Zhu C M. 1985. High pressure fusion curve of alloys $Ni_{70}Mn_{30}$, $Ni_{40}Mn_{30}Fe_{30}$ and $Ni_{70}Mn_{25}Co_5$ used in synthesizing diamonds (in Chinese). J Chin Silicate Solicate, 13: 381–384

Gao S, Rudnick R L, Yuan H L, et al. 2004. Recycling lower continental crust in the North China Craton. Nature, 432: 892–897

Gao S, Rudnick R L, Xu W L, et al. 2008. Recycling deep cratonic lithosphere and generation of intraplate magmatism in the North China Craton. Earth Planet Sci Lett, 270: 41–53

Gao S, Zhang J F, Xu W L, et al. 2009. Delamination and destruction of the North China Craton. Chin Sci Bull, 54: 1962–1973

Gong C Y, Liu Y G, Li P, et al. 2011. Comparison of measurement methods for electrical conductivity of rocks under high pressure and high temperature: Taken the lherzolite as an example (in Chinese). Acta Geol Sin, 85: 243–253

Grove T L. 1981. Use of FePt alloys to eliminate the iron loss problem in 1 atmosphere gas mixing experiments: Theoretical and practical considerations. Contrib Mineral Petrol, 78: 298–304

Huang H, Gao S, Hu Z C, et al. 2007. Geochemistry of the high-Mg andesites at Zhangwu, western Liaoning: Implication for delamination of newly formed lower crust. Sci China Ser D-Earth Sci, 37: 1287–1300

Johnston A D, Wyllie P J. 1989. The system tonalite-peridotite-H_2O at 30 kbar, with applications to hybridization in subduction zone magmatism. Contrib Mineral Petrol, 102: 257–264

Kelemen P B. 1995. Genesis of high Mg# andesites and the continental crust. Contrib Mineral Petrol, 120: 1–19

Liang Y. 2010. Multicomponent diffusion in molten silicates: Theory, experiments, and geological applications. Rev Miner Geochem, 72: 409–446

Liu Y S, Gao S, Lee C, et al. 2005. Melt-peridotite interactions: Links between garnet pyroxenite and high-Mg# signature of continental crust. Earth Planet Sci Lett, 234: 39–57

Pearce J A, Laan S R V D, Arculus R J, et al. 1992. Boninite and harzburgite from leg 125 (Bonin-Mariana forearc): A case study of magma genesis during the initial stages of subduction. Proc Ocean Drill Prog Sci Results, 125: 623–659

Rapp R P, Shimizu N, Norman M D, et al. 1999. Reaction between slab-derived melts and peridotite in the mantle wedge experimental constraints at 3.8 GPa. Chem Geol, 160: 335–356

Sekine T, Wyllie P J. 1982. The system granite-peridotite-H_2O at 30 kbar, with applications to hybridization in subduction zone magmatism. Contrib Mineral Petrol, 81: 190–202

Shimoda G, Tatsumi Y, Nohda S, et al. 1998. Setouchi high-Mg andesites revisited: Geochemical evidence for melting of subducting sediments. Earth Planet Sci Lett, 160: 479–492

Wang C, Jin Z M, Gao S, et al. 2010. Eclogite-melt/peridotite reaction: Experimental constrains on the destruction mechanism of the North China Craton. Sci China Earth Sci, 40: 541–555

Wang X R, Gao S, Liu X M, et al. 2005. Geochemistry of high-Mg andesites from the early Cretaceous Yixian Formation, western Liaoning: Implications for lower crustal delamination and Sr/Y variations. Sci China Ser D-Earth Sci, 35: 700–709

Wu X Y, Xu Y G, Ma J L, et al. 2003. Geochemical and petrogeneis of the Mesozoic high-Mg diorite from westen Shandong (in Chinese). Geotectonica et Metallogenia, 27: 228–236

Xie H S, Hou W, Zhou W G. 2005. Water content in the Earth's mantle (in Chinese). Earth Sci Front, 12: 55–60

Xiong X L, Liu X C, Zhu Z M, et al. 2011. Adakitic rocks and destruction of the North China Craton: Evidence from experimental petrology and geochemistry. Sci China Earth Sci, 54: 858–870

Xu W L, Hergt J M, Gao S, et al. 2008. Interaction of adakitic melt-peridotite: Implications for the high-Mg# signature of Mesozoic adakitic rocks in the eastern North China Craton. Earth Planet Sci Lett, 265: 123–137

Xu W L, Yang C H, Yang D B, et a1. 2006. Mesozoic high-Mg diorites in eastern North China craton: Constraints on the mechanism of lithospheric thinning (in Chinese). Earth Sci Front, 13: 120–129

Xu Y G. 1993. Geothermometers applicable to the mantle xenoliths (in Chinese). Acta Petrol Sin, 9: 167–180

Xu Y G. 2001. Thermo-tectonic destruction of the Archaean lithospheric keel beneath the Sino-Korean Craton in China: Evidence, tming and mechanism. Phys Chem Earth, 26: 747–757

Yu Y, Xu W L, Liu X Y, et al. 2009. Amphibole garnet pyroxenite-peridotite reaction under the conditions of high temperature and high pressure: Preliminary experimental results and their geological significance (in Chinese). Prog Nat Sci, 19: 644–651

Yuan H L, Liu X M, Liu Y S, et al. 2005. Geochemistry and U-Pb zircon geochronology of Late-Mesozoic lavas from Xishan, Beijing. Sci China Ser D-Earth Sci, 35: 821–836

Zhang H F, Sun M, Zhou X H, et al. 2003. Secular evolution of the lithosphere beneath the eastern North China Craton: Evidence from Mesozoic basalts and high-Mg andesites. Geochim Cosmochim Acta, 67: 4373–4387

Zhang Q, Wang Y, Qiang Q, et al. 2001. The characteristics and tectonic-metallogenic significances of the adakites in Yanshan period from eastern China (in Chinese). Acta Petrol Sin, 17: 236–244

Zhang W L, Shao J A, Wang R C, et al. 2011. Sr-rich apatite from the Dangzishan leucitite-ijolite xenoliths (Heilongjiang Province): Mineralogy and mantle-fluid metasomatism. Chin Sci Bull, 56: 53–63